Adaptivity of Voltage-Controlled Oscillators—Theory and Design

Aleksandar Tasić, Wouter A. Serdijn, and John R. Long

***Abstract*—Analog RF front-end circuits are typically designed to perform one specific task, while key parameters such as dynamic range, bandwidth and selectivity are fixed by the hardware design and not by the communication system in an adaptive way. As a result, today's receiver topologies are designed to function under the most stringent conditions, which increases circuit complexity and power consumption. However, the conditions under which the RF circuits operate are not fixed but vary widely and depend upon a multitude of factors. Therefore, a concept of design for adaptivity is introduced in this paper. It establishes a trajectory for an all-round performance characterization of adaptive oscillators with an explicit qualitative and quantitative description of all the existing relations and tradeoffs among the oscillator performance parameters. As a proof of concept, an 800-MHz adaptive voltage-controlled oscillator is designed with phase-noise tuning range of 7 dB and more than a factor 3 saving in power consumption, suitable for unobtrusive mobile equipment, foreseen to operate in this band.**

***Index Terms*—Adaptive circuits, analog circuits, loop gain, low-power integrated circuit (IC) design, phase-noise tuning, RF circuits, voltage-controlled oscillators (VCOs).**

I. Introduction

WIRELESS telecommunication transceivers should be broadband, low power, and adaptive. Broad bandwidth supports high data rates demanded by emerging applications. Adaptivity accommodates varying channel conditions and user and application requirements, while consuming as little energy as possible ensures long talk times on one battery charge.

While aspects of broadband and low-power RF circuit design have been addressed [1], [2], the issue of adaptivity has not progressed further than switching between different circuits. This approach is simple to implement, but is neither optimal in cost nor power consumption [3]. However, by sharing functional blocks, adaptive RF front-end circuits offer reduced complexity, chip area and over-all cost.

Many parameters and figures of merit characterizing the performance of voltage-controlled oscillators (VCOs) have been introduced, but the interaction and design tradeoffs between theses metrics are often unclear [4], [5]. Therefore, explicit qualitative and quantitative descriptions [6], [7] of the existing relationships and tradeoffs between VCO performance parameters are outlined in this paper.

The adaptivity phenomena of oscillators are introduced in the following section. Section III describes phase-noise performance of an adaptive quasi-tapped (QT) bipolar VCO. Adaptivity figures of merit, viz., phase-noise tuning range and frequency-transconductance sensitivity are derived in Section IV. A proof-of-concept design example is outlined in Section V, while Section VI summarizes the conclusions.

Manuscript received April 1, 2004; revised July 9, 2004 and October 5, 2004. This paper was recommended by Associate Editor B. Maundy.

The authors are with the Electronics Research Laboratory/DIMES, Delft University of Technology, Delft 2628CD, The Netherlands (e-mail: a.tasic@ewi.tudelft.nl).

Digital Object Identifier 10.1109/TCSI.2005.846223

II. Adaptivity Phenomena of Oscillators

The importance of low-voltage and low-power design has resulted in the design of circuits operating at the very edge of the required performance. Generally, analog RF front-end circuit designs are aimed at fulfilling a set of specifications resulting from specific, worst-case radio-channel conditions. However, the fact that radio channels are not fixed but rather variant must be taken into account in the design of RF circuits. *Design for adaptivity* [8] is suitable for mobile equipment that supports various services and operate with variable workloads in a variety of environments.

Design for adaptivity of oscillators encompasses phase-noise tuning and frequency-transconductance tuning phenomena.

A. Phase-Noise Tuning

If the radio-channel conditions improve (or a relaxed communication standard is active), poorer phase noise of oscillators can be tolerated, leading to power savings. Responding to such a new situation, design for adaptivity appears to be a solution as a standard, fixed design is "blind" and "deaf" for volatile specifications set by communication systems.

By trading phase noise for power consumption, oscillators and oscillating systems can be adapted to varying conditions and also satisfy the requirements of the complete RF front-end system. The concept of phase-noise tuning [6] shows explicitly how phase noise and power consumption trade between each other in an adaptive way.

The analytical description of this adaptivity phenomenon is presented in Section IV.

B. Frequency-Transconductance Tuning

The design of low-power VCOs is usually aimed at a loop gain slightly larger than the necessary minimum of one (e.g., two). In such cases, an increase in the capacitance of the oscillator's LC-tank varactor in order to lower the oscillation frequency results in an increase of the effective tank conductance. If the design is "fixed" rather than adaptive, the oscillation condition deteriorates as the loop gain is lowered. Accordingly, this can bring an RF front-end to a halt, as there might be no oscillations.

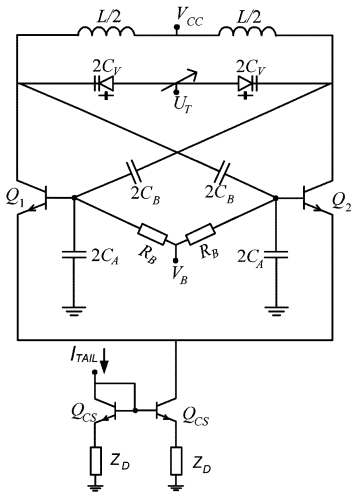

Fig. 1. QT *LC* oscillator.

In situations where power consumption is of less concern than oscillator phase noise, the repercussions are different but not less detrimental. In such situation, the oscillation condition is rather relaxed, as the loop gain can be much larger than two. However, the voltage swing across the *LC* tank will be reduced due the increase in the effective tank conductance (increased varactor capacitance), resulting in a worse phase noise performance.

In both of these examples, the oscillator could still fulfill the requirements if the bias conditions of the oscillator were adapted. Thus, *frequency-transconductance* $(C{-}g_m)$ tuning [7] is the control mechanism compensating for the change in the VCO *LC*-tank characteristic, i.e., its conductance is changed due to frequency tuning, by varying the oscillator's bias conditions (control of active part transconductance).

A figure of merit related to this adaptivity phenomenon is analytically described in Section IV.

III. Phase-Noise Performance of Quasi-Tapped VCOs

The QT bipolar VCO [9] shown in Fig. 1 is used to implement the adaptive oscillator. It consists of a resonating *LC* tank and a cross-coupled transconductance amplifier (Q_1, Q_2), with a tank inductance L, a tank varactor capacitance C_V, and quasi-tapping capacitances C_A and C_B. The bias source provides current I_{TAIL} and includes degenerative impedance Z_D.

Feedback via tapped capacitors C_A and C_B has a manifold role. First, it maximizes the voltage swing across the *LC* tank, while active devices Q_1 and Q_2 remain far from heavy saturation. Moreover, freedom to set base bias V_B lower than the supply voltage V_{CC} allows for a large tank voltage. Finally, capacitances C_A and C_B allow for a direct coupling of the oscillation signal (oscillator) with the interfacing circuitry, obviating the need for decoupling capacitors.

The quasi-tapping capacitances C_A and C_B serve to define the quasi-tapping ratio and not only to facilitate biasing of the transistors in the active part of the oscillator. The quasi-tapping capacitances C_A and C_B determine the *performance* of the oscillator under consideration, being phase noise and power consumption, *equally* with other elements in the circuitry.

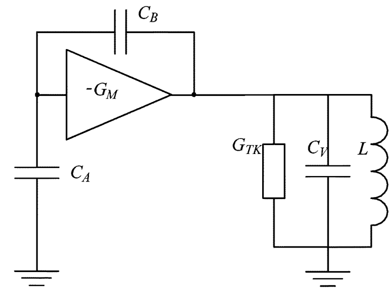

Fig. 2. Simplified model of a QT oscillator.

The relationship between the parameters of the oscillator can be summarized as

$$G_{\text{TK}} = \frac{R_L}{(\omega_0 L)^2} + R_C(\omega_0 C_V)^2 \tag{1}$$

$$n = 1 + \frac{C_A}{C_B} \quad G_M = \frac{g_m}{2}$$

$$G_{M,\text{TK}} = \frac{G_M}{n} \quad g_m = \frac{I_{\text{TAIL}}}{2V_T} \tag{2}$$

$$L_{\text{TOT}} = L \quad C_{\text{TOT}} = C_V + \frac{C_A C_B}{C_A + C_B}$$

$$\omega_0 = \frac{1}{\sqrt{L_{\text{TOT}} C_{\text{TOT}}}}. \tag{3}$$

Here, R_L and R_C stand for the inductor L and the varactor C_V series loss resistances, G_{TK} the effective tank conductance, n the quasi-tapping factor, $-G_M$ the small-signal transconductance of the active part of the oscillator, $-G_{M,\text{TK}}$ the small-signal conductance seen by the *LC* tank, g_m the transconductance of the bipolar transistors and V_T the thermal voltage.

A simplified model of the QT oscillator is shown in Fig. 2. In this second-order[1] negative-resistance oscillator, the oscillation condition is satisfied when the equivalent *LC*-tank loss G_{TK} is compensated by the equivalent negative small-signal transconductance of the active part $-G_M$, after being transformed to the resonating tank over the quasi-tapping capacitances, i.e., $G_{M,\text{TK}} \geq G_{\text{TK}}$. The condition $G_{M,\text{TK}} = G_{\text{TK}}$ is referred to as start-up condition of the oscillations, whereas the condition $G_{M,\text{TK}} \geq G_{\text{TK}}$ is referred to as safety start-up condition (e.g., $G_{M,\text{TK}} = 2G_{\text{TK}}$).

A. Noise Analysis

In the following analysis, it is assumed that the oscillator operates in a near-linear fashion such that the original noise close to the carrier contributes to a greater extent to the total oscillator noise, compared to the other contributors, such as baseband noise and the noise obtained after mixing from other harmonics.

The oscillator phase-noise performance depends mainly on the components in the ac signal path, i.e., the transconductance cell and resonator, when noise contributed by the bias circuit is made negligible [11]. Moreover, as near-linear operation assumes simultaneously active transconductor devices Q_1 and Q_2, noise from the tail-current source, being a common-mode

[1]Even though the QT VCO resembles a differential version of the Colpitts oscillator, [10], there are two fundamental differences: 1) the Colpitts VCO is a third-order harmonic oscillator and 2) it has optimal performance for a tapping ratio (n) equal to 5.

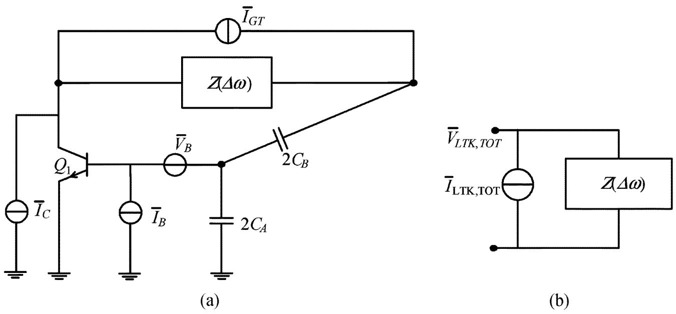

Fig. 3. Noise analysis. (a) Noisy oscillator model (left). (b) Noisy tank model (right).

signal, can indeed be neglected from the analysis. Used for *qualitative inspection* of the oscillators' phenomena, these assumptions enable easier interpretation [12] of the rather complex noise generating mechanism in oscillators.

The main noise sources of the oscillator under consideration are shown in Fig. 3(a). In order to switch to the equivalent model of Fig. 3(b), it is necessary to transform the indicated noise sources to the corresponding *LC* tank, $Z(\Delta\omega)$. For the sake of brevity, and because of symmetry, only one half of the oscillator is depicted. However, in the following calculations, the complete oscillator is analyzed.

Considered uncorrelated, all noise sources [Fig. 3(a)] add to the equivalent noise source $\bar{I}_{\mathrm{LTK,TOT}}$ as given by (4) and Fig. 3(b)

$$\bar{I}^2_{\mathrm{LTK,TOT}} = \bar{I}^2_{\mathrm{LTK},GT} + \bar{I}^2_{\mathrm{LTK},IB} + \bar{I}^2_{\mathrm{LTK},IC} + \bar{I}^2_{\mathrm{LTK},VB}. \quad (4)$$

The corresponding "near-linear" noise contributions equal

$$\bar{I}^2_{\mathrm{LTK},VB} = 2\bar{V}^2_B n^2 G^2_{\mathrm{TK}}, \qquad \bar{V}^2_B = 4KTr_B \quad (5)$$
$$\bar{I}^2_{\mathrm{LTK},IB} = \bar{I}^2_B/2n^2, \qquad \bar{I}^2_B = 2qI_B \quad (6)$$
$$\bar{I}^2_{\mathrm{LTK},IC} = 1/2\bar{I}^2_C, \qquad \bar{I}^2_C = 2qI_C \quad (7)$$
$$\bar{I}^2_{\mathrm{LTK},GT} = 4KTG_{\mathrm{TK}}. \quad (8)$$

$\bar{I}_B$ is the base current shot noise, $\bar{I}_C$ the collector current shot noise and $\bar{V}_B$ the base resistance r_B thermal noise. I_C and I_B stand for the collector and base currents of the transconductor transistors, respectively.

Given the tank impedance $Z(\Delta\omega)$,

$$Z(\Delta\omega) \cong \frac{-j\omega_0 L}{2\Delta\omega/\omega_0} \quad (9)$$

the voltage-noise spectral density across the *LC* tank equals

$$\begin{aligned}\bar{V}^2_{\mathrm{LTK,TOT}} &= \bar{I}^2_{\mathrm{LTK,TOT}}|Z(\Delta\omega)|^2 \\ &= KT\frac{G_{\mathrm{TK}}}{(\omega_0 C_{\mathrm{TOT}})^2}(1+A_T)\left(\frac{\omega_0}{\Delta\omega}\right)^2 \quad (10)\end{aligned}$$

$$A_T = 2n^2 r_B G_{\mathrm{TK}} + \frac{g_m}{4G_{\mathrm{TK}}}\left(1+\frac{1}{\beta n^2}\right). \quad (11)$$

From (2) and assuming $\beta \gg 1$, the noise factor of the active part $A_{T,S-\mathrm{UP}}$ for the start-up condition $(G_{M,\mathrm{TK}} = G_{\mathrm{TK}})$, simplifies to

$$A_{T,S-\mathrm{UP}} = n\left(\frac{1}{2} + r_B g_{\mathrm{ms-up}}\right) \quad (12)$$

or for the reliable (safety) start-up condition $(G_{M,\mathrm{TK}} > G_{\mathrm{TK}})$, corresponding to the case with an excess small-signal loop gain (k) larger than one (e.g., $k = 2$), it is given as

$$\begin{aligned}A_{T,S\_S-\mathrm{UP}} &= n\left(\frac{k}{2} + \frac{r_B g_{\mathrm{ms\_s-up}}}{k}\right) \\ &= n\left(\frac{k}{2} + r_B g_{\mathrm{ms-up}}\right). \quad (13)\end{aligned}$$

Indexes $S-\mathrm{UP}$ and $S\_S-\mathrm{UP}$ correspond to the start-up and the safety start-up conditions of the oscillations.

B. Phase Noise of QT VCOs

Phase noise $\mathcal{L}$ of an oscillator is defined as the ratio of the noise power in a 1-Hz bandwidth at a frequency $f_0 + \Delta f$, and the carrier power

$$\mathcal{L} = \frac{\bar{V}^2_{\mathrm{LTK,TOT}}}{v^2_{S,\mathrm{QT}}}. \quad (14)$$

$\bar{V}^2_{\mathrm{LTK,TOT}}$ is the total voltage-noise spectral density (10) at the output of the oscillator (*LC*-tank) and $v_{S,\mathrm{QT}}$ is the amplitude of the voltage swing across the *LC* tank. Index QT refers to QT oscillators.

As the noise parameters have already been derived, yet the amplitude $v_{S,\mathrm{QT}}$ of the oscillation signal has to be determined in order to calculate the phase noise of the QT VCO.

Defined as product of the equivalent tank resistance at the resonant frequency $(1/G_{\mathrm{TK}})$ and the first Fourier coefficient of the current sensed by the *LC* tank, the voltage swing across the tank equals

$$v_{S,\mathrm{QT}} = \frac{2}{\pi}\frac{I_{\mathrm{TAIL}}}{G_{\mathrm{TK}}}. \quad (15)$$

With the aid of (2), the start-up voltage swing $v_{S,S-\mathrm{UP,QT}}$ over the *LC* tank becomes

$$v_{S,S-\mathrm{UP,QT}} = \frac{8}{\pi}nV_T \quad (16)$$

or for an arbitrary k-times increase in power (loop gain), $v_{S,\mathrm{QT}}$ equals

$$v_{S,\mathrm{QT}} = \frac{8}{\pi}nkV_T \quad (17)$$

Now, with the aid of (11), (13), (14), and (17), the phase-noise model of a QT oscillator becomes

$$L_{\mathrm{QT}}(k) \propto \frac{1 + n\cdot(k/2 + r_B g_{\mathrm{ms-up,QT}})}{k^2 n^2}. \quad (18)$$

This model is parameterized with respect to power consumption via the *small-signal loop gain* k defined as

$$k = \frac{G_{M,\mathrm{TK}}}{G_{\mathrm{TK}}}. \quad (19)$$

Also, k refers to the excess of the negative conductance necessary for the compensation of the losses in the *LC* tank. Namely, if the tank conductance is G_{TK}, then for the start-up of the oscillations the equivalent negative conductance seen by the tank must be $G_{M,\mathrm{TK}} = kG_{\mathrm{TK}}$, where k is larger than one, for the safety start-up usually set to a value of two. The linear phase-noise model (18) is used for analysis of VCOs with lower loop-gain values, as they can be assumed to operate in near-linear fashion.

C. Phase-Noise Ratio

The performance of the QT VCO will be characterized by comparing a QT VCO to an oscillator with a different quasi-tapping factor, e.g., a VCO with $n = 1$. Called a nontapped (NT) VCO, it is an oscillator with directly coupled *LC* tank and active part (i.e., the oscillator shown in Fig. 1 with $C_B = \infty$ and $C_A = 0$). The *LC* tanks of both oscillator types are assumed identical.

With the aid of (18) and for an arbitrary distance from the start-up condition, the phase noise of a QT VCO and an NT-VCO ($n = 1$) can be written as

$$L_{\rm QT} \propto \frac{1 + n \cdot (k/2 + c_{\rm QT})}{n^2 k^2} \tag{20}$$

$$L_{\rm NT} \propto \frac{1 + k/2 + c_{\rm NT}}{k^2} \tag{21}$$

where $c_{\rm QT} = nc_{\rm NT} = nr_B g_{\rm ms-up,NT}$, with $g_{\rm ms-up,NT}$ being the start-up ($k_{\rm NT} = 1$) small-signal transconductance of an NT-VCO. Letting $A_{\rm NT}(k) = k/2 + c_{\rm NT}$, the corresponding phase-noise formulae transform into

$$L_{\rm QT}(k) \propto \frac{1 - (n-1) \cdot n \cdot k/2 + A_{\rm NT}(k) n^2}{n^2 k^2} \tag{22}$$

$$L_{\rm NT}(k) \propto \frac{1 + A_{\rm NT}(k)}{k^2}. \tag{23}$$

Now, the *ratio* between the *phase noise* of a nontapped oscillator and a QT oscillator $\mathrm{PNR}(k_{\rm QT}, k_{\rm NT})$, can be defined as

$$\mathrm{PNR}(k_{\rm QT}, k_{\rm NT}) = \frac{L_{\rm NT}(k_{\rm NT})}{L_{\rm QT}(k_{\rm QT})} \tag{24}$$

$$\mathrm{PNR}(k_{\rm QT}, k_{\rm NT}) = \frac{2n^2 k_{\rm QT}^2 [1 + A_{\rm NT}(k_{\rm NT})]}{2 - (n-1) \cdot n \cdot k_{\rm QT} + 2n^2 A_{\rm NT}(k_{\rm QT})} \frac{1}{k_{\rm NT}^2}. \tag{25}$$

For $n = 1$ and $k_{\rm NT} = k_{\rm QT}$, the QT VCO reduces to the NT-VCO, and obviously, the ratio PNR becomes equal to one.

The operating conditions that are used for the comparison of oscillators are the same power consumption condition ($k_{\rm NT} = nk_{\rm QT}$), and the same distance from the start-up condition (i.e., the same loop gain, $k_{\rm NT} = k_{\rm QT} = k$). The latter because loop gain is an important oscillator parameter. Without loss of generality, and for easier interpretation, we will assume that the quasi-tapping factor equals two, $n = 2$.

From (25), the phase-noise ratio for the same power consumption ($k_{\rm NT} = 2k_{\rm QT} = 2k$) equals

$$\mathrm{PNR}(k, 2k) = \frac{1 + A_{\rm NT}(2k)}{1 - k + 4A_{\rm NT}(k)} = \frac{1 + k + c_{\rm NT}}{1 + k + 4c_{\rm NT}} < 1. \tag{26}$$

As expected, a nontapped oscillator has better performance than a QT oscillator, with respect to the phase noise for the same power consumption. For example, if $k_{\rm NT} = 1$ (the start-up condition), $r_B = 40\ \Omega$ and $g_{ms-{\rm up,NT}} = 4.1$ mS, there is a difference in phase noise of $\mathrm{PNR} = 0.8$ dB in favor of the nontapped oscillator.

In a similar manner, the phase-noise ratio for the same excess negative conductance ($k_{\rm NT} = k_{\rm QT} = k$) is given as

$$\mathrm{PNR}(k, k) = \frac{4 + 4A_{\rm NT}(k)}{1 - k + 4A_{\rm NT}(k)} = \frac{4 + 2k + 4c_{\rm NT}}{1 + k + 4c_{\rm NT}} > 1. \tag{27}$$

This result shows that a QT oscillator has better performance than a nontapped oscillator, with respect to the phase noise for the same loop gain. Referring to the same example and $k = 6$ [6], there is a difference of $\mathrm{PNR} = 3.4$ dB in favor of a QT oscillator.

Finally, we can conclude that the QT VCO with $V_B < V_{\rm CC}$ (Fig. 1) and the quasi-tapping ratio n close to one offers the most design flexibility as it allows for the increased voltage swing across the *LC* tank ($V_B < V_{\rm CC}$) and improved phase noise accordingly as well as for reduced power consumption ((26), $n = 1$).

IV. Adaptivity Figures of Merit

Adaptivity phenomena can be qualitatively and quantitatively described by means of their figures of merit [13]. Phase-noise tuning range describes phase-noise adaptivity of an oscillator with respect to power consumption. Frequency-transconductance sensitivity describes compensation of the change in the *LC* tank characteristic due to frequency tuning. Both metrics are analytically derived in the remainder of this section.

A. Phase-Noise Tuning Range

Before the phase noise adaptivity metric is described, let us broaden the meaning of the corner-stone parameter k. In the oscillator under consideration, the start-up condition is also referred to the minimum power condition. Apart from defining how far the oscillator is from this state, parameter k also characterizes the increase in power. Namely, a k-times larger negative conductance of the active part of the oscillator requires a k-times increase in power in order to sustain the same loop gain (power consumption is controlled by the tail current $I_{\rm TAIL}$, shown in Fig. 1).

Whereas the phenomenon of the adaptation of oscillator's phase noise to different conditions and specifications is named phase-noise tuning, the figure of merit describing the oscillator's adaptivity to phase noise is named the *phase-noise tuning range* (PNTR). For a k_2/k_1-times change in power consumption, the phase-noise tuning range of the QT VCO (Fig. 1) is, with the aid of (18), defined as

$$\mathrm{PNTR}(k_1, k_2) = \frac{\mathcal{L}_{\rm QT}(k_1)}{\mathcal{L}_{\rm QT}(k_2)} = \frac{k_2^2}{k_1^2} \frac{1 + n(k_1/2 + c)}{1 + n(k_2/2 + c)} \tag{28}$$

where $c = c_{\rm QT}$.

If the guaranteed (safety) start-up condition corresponds to $k_{\rm MIN} = 2$, in order to estimate the achievable phase-noise tuning range, the loop gain $k_{\rm MAX}$, related to the best phase noise, will be determined first.

For the maximum voltage swing across the *LC* tank that satisfies

$$v_{S,\mathrm{QT,MAX}} \leq \frac{2n}{n+1}(V_{\mathrm{CC}} - V_B + V_{\mathrm{BE}} - V_{\mathrm{CE,SAT}}) \quad (29)$$

the detrimental effects of both hard saturation of the transconductor transistors Q_1 and Q_2, and the additional current-noise of their forward biased base-collector junctions can be circumvented [14]. Here, V_{CC} is the supply voltage, V_B the base potential of transistors Q_1 and Q_2, V_{BE} their base–emitter voltage and $V_{\mathrm{CE,SAT}}$ their collector–emitter saturation voltage.

Assuming that the bases of the transistors are, for the sake of the simplicity, at the maximum supply voltage, i.e., $V_{\mathrm{CC}} = V_B$, the maximum voltage swing across the *LC* tank ($V_{\mathrm{CE,SAT}} = 0$ V) equals $v_{S,\mathrm{QT,MAX1}} = 1.5n/(n+1)$ (it is assumed that $V_{\mathrm{BE}} = 0.75$ V). On the other hand, the maximum voltage swing corresponding to the nonsaturation condition ($V_{\mathrm{CE,SAT}} = 0.3$ V) is calculated from (29) as $v_{S,\mathrm{QT,MAX2}} = 0.9n/(n+1)$. Compromising between larger voltage swing ($v_{S,\mathrm{QT,MAX1}}$) on the one hand and weaker saturation on the other ($v_{S,\mathrm{QT,MAX2}}$), we opt for a maximum voltage swing across the tank that equals

$$v_{S,\mathrm{QT,MAX}} = \frac{v_{S,\mathrm{QT,MAX1}} + v_{S,\mathrm{QT,MAX2}}}{2}. \quad (30)$$

Now, with the aid of (17) and (30), and for $n = 2$, the maximal loop-gain value is found to be $k_{\mathrm{MAX}} = 6$.

For example, if $k_{\mathrm{MIN}} = 2$ (the safety start-up condition) and $k_{\mathrm{MAX}} = 6$ (expected best phase noise), $r_B = 40\ \Omega$ and $g_{m,S-\mathrm{UP,QT}} = 8.2$ mS, the PNTR for a quasi-tapping factor $n = 2$ equals

$$\mathrm{PNTR}(2,6)[\mathrm{dB}] = 10 \log \frac{\mathcal{L}_{\mathrm{MIN}}}{\mathcal{L}_{\mathrm{MAX}}} = 6.3 \quad (31)$$

where $\mathcal{L}_{\mathrm{MAX}}$ and $\mathcal{L}_{\mathrm{MIN}}$ represent the maximum and the minimum phase noise corresponding to the values of k_{MAX} and k_{MIN}, respectively.

The obtained result shows that for the oscillator under consideration (equal supply and base bias voltages), a phase-noise tuning range around 6 dB can be expected with a factor 3 change in power consumption.

B. Frequency-Transconductance Sensitivity

Because of a change in frequency due to tuning of the *LC*-tank varactor capacitance (C_V), the loop gain, the voltage swing and the phase noise of the oscillator change as well [15]. If the oscillator is designed at the very edge of the required specifications, the change of the oscillation condition (i.e., reduced loop gain), or the change of the noise produced (i.e., degraded phase noise), puts the oscillator out of correct operation. In order to preserve desired operation of oscillators, it is necessary to apply a control mechanism to the bias current I_{TAIL} (i.e., g_m).

The concept of $C{-}g_m$ tuning illustrates the relationship between the varactor diode tuning voltage U_T and the biasing tail current I_{TAIL}, both indicated in Fig. 1. The objective is to find the relationship between the tuning voltage U_T and the effective tank conductance G_{TK} on the one hand and the relationship between the tank conductance and the biasing tail current I_{TAIL} on the other. The resulting sensitivity of the tail current to the tuning voltage will show to what extent the biasing condition should be changed in response to a change in the frequency, in order to keep the oscillator operating under the specified conditions.

The sensitivity of the *LC*-tank conductance to a change in a tuning voltage is defined as

$$S_{U_T}^{G_{\mathrm{TK}}}\Big|_{U_T=U_{T0}} = \frac{\partial G_{\mathrm{TK}}}{\partial C_V}\frac{\partial C_V}{\partial U_T} \quad (32)$$

where tuning voltage U_{T0} corresponds to the resonant frequency f_0.

With the aid of (1) and (3), the sensitivity of the *LC*-tank conductance to a change in varactor capacitance C_V can be expressed in terms of *LC*-tank parameters

$$S_{C_V}^{G_{\mathrm{TK}}} = \omega_0^2 \left[2C_V R_C \left(1 - \frac{C_V}{2C_{\mathrm{TOT}}}\right) + C_{\mathrm{TOT}} R_L\right]. \quad (33)$$

If the varactor capacitance is related to a tuning voltage U_T as

$$C_V(U_T) = \frac{C_{V0}}{\left(1 + \frac{V_{\mathrm{CC}} - U_T}{\varphi}\right)^{1/a}} \quad (34)$$

where C_{V0}, φ, and a are the parameters of the varactor shown in Fig. 1, the sensitivity of the varactor capacitance to a tuning voltage equals

$$S_{U_T}^{C_V} = \frac{C_V}{a(V_{\mathrm{CC}} - U_{T0} + \varphi)}. \quad (35)$$

Note that the capacitance C_V is related to the tuning voltage U_{T0} and the frequency f_0.

Linearizing the calculated sensitivity characteristics around resonance, the change in the effective tank conductance can be related to the change in the tuning voltage as

$$\Delta G_{\mathrm{TK}} = S_{U_T}^{G_{\mathrm{TK}}} \Delta U_T \quad (36)$$

where the relating sensitivity has a form

$$S_{U_T}^{G_{\mathrm{TK}}} = \frac{2(\omega_0 C_V)^2}{a(V_{\mathrm{CC}} - U_{\mathrm{TO}} + \varphi)} \times \left[R_C\left(1 - \frac{C_V}{2C_{\mathrm{TOT}}}\right) + \frac{C_{\mathrm{TOT}} R_L}{2C_V}\right]. \quad (37)$$

To compensate for such a change in the tank characteristic, the conductance seen by the tank ($-G_{M,\mathrm{TK}}$) should be changed by the same amount. From (2), the relationships between the tail current, the transconductance and the conductance converted to the *LC* tank are determined

$$\Delta I_{\mathrm{TAIL}} = 2V_T \Delta g_m \quad (38)$$

$$\Delta g_m = 2 \cdot \Delta G_{M,\mathrm{TK}}. \quad (39)$$

Combining these results, the change in the tail current relates to the change in the absolute value of the conductance seen by the *LC* tank as

$$S_{G_{M,\mathrm{TK}}}^{I_{\mathrm{TAIL}}} = 4n \cdot V_T. \quad (40)$$

Satisfying the condition [see (19)]

$$\Delta G_{M,\mathrm{TK}} = k \Delta G_{\mathrm{TK}} \quad (41)$$

the sensitivity of the tail current to the tuning voltage, referred to the increase or the reduction in the tail current (power consumption) in order to sustain the desired loop-gain value (oscillation condition) is calculated as

$$S_{U_T}^{I_{\rm TAIL}} = S_{G_{M,\rm TK}}^{I_{\rm TAIL}} S_{G_{\rm TK}}^{G_{M,\rm TK}} S_{U_T}^{G_{\rm TK}}. \tag{42}$$

With the aid of (37), (40), (41), and (42), we finally obtain

$$S_{U_T}^{I_{\rm TAIL}} = \frac{8k \cdot n \cdot V_T(\omega_0 C_V)^2}{a(V_{\rm CC} - U_{\rm T0} + \varphi)} \times \left[R_C\left(1 - \frac{C_V}{2C_{\rm TOT}}\right) + \frac{C_{\rm TOT}R_L}{2C_V}\right]. \tag{43}$$

For the oscillator under consideration this expression allows one to estimate to what extent the tail current should be changed, as a result of a change in the tuning voltage (i.e., frequency), in order to keep the oscillator operating under the required conditions.

For example, for $f_0 = 900$ MHz, $2C_V = 2$ pF, $Q_C = 15$, $L/2 = 12.5$ nH, $Q_L = 4$, $2C_A = 1$ pF, $2C_B = 1$ pF, $V_{\rm CC} = 2$ V, $U_{T0} = 1$ V, $\varphi = 0.5$ V, $a = 2$, and $k = 2$, where Q_C and Q_L are the quality factors of the corresponding varactors and inductors, the sensitivity $S_{U_T}^{I_{\rm TAIL}} = 0.25$ mA/V results. It infers that in order to sustain the oscillations under the same condition (i.e., the same loop gain) the tail current should be either increased or reduced (depending on the direction of the frequency tuning) by 0.25 mA for a 1-V change in a varactor voltage. The counterpart of the $C - gm$ tuning in the circuitry is a simple amplitude control mechanism, as constant loop gain means constant amplitude of the signal across the *LC* tank of the oscillator.

V. Application of Design for Adaptivity

Single-mode, single-standard oscillators are conventionally designed to satisfy the most stringent conditions, having all the performance and circuit parameters fixed. As in portable devices, e.g., unobtrusive electronics equipment, the RF front-end circuits are exposed to such conditions only for a short period of time during operation, this (over)design for worst case conditions turns out to be rather expensive in terms of power consumption. However, *circuit adaptation* to varying channel conditions and application requirements ensures lower cost as the adaptivity allows for considerable power savings as well as longer battery life.

Selection of design parameters of an adaptive oscillator circuit is different from the design for a fixed performance. The phase-noise adaptivity figure of merit (28) that accounts for a number of oscillator operation conditions and required specifications forms a base for design of adaptive oscillators. Namely, for given PNTR, the maximum loop gain ($k_{\rm MAX}$) can be determined from (28) (the minimum loop gain is already known, e.g., $k_{\rm MIN} = 2$). On the other hand, if the maximum and the minimum loop gain values are know, the obtainable PNTR can be determined from (28) (i.e., the range of oscillator adaptation with respect to the phase noise).

Furthermore, from the maximum phase-noise requirements and frequency tuning range requirement, the *LC*-tank parameters can be determined, i.e., coil inductance and varactor capacitance. Once the resonator components are known, the equivalent tank conductance ($G_{\rm TK}$) and the minimum power consumption (current $I_{\rm TAIL,MIN}$) can be determined from (1) and (2), respectively.

Finally, from the maximum loop gain on the one hand and the minimum tail current on the other, the maximum power consumption (tail current) can be found, providing an oscillator with the required phase-noise tuning range.

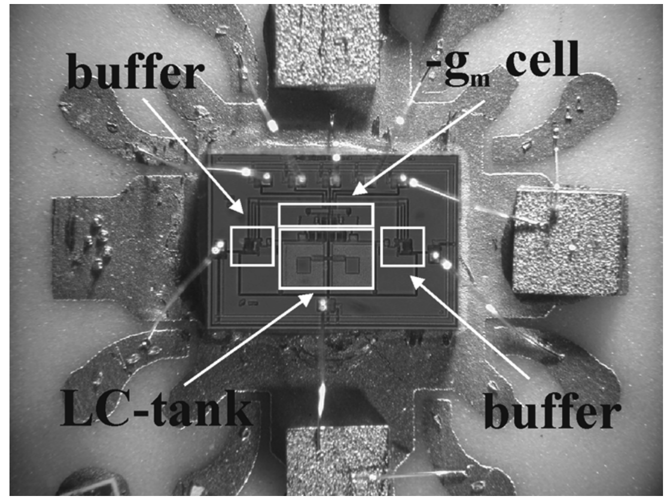

Fig. 4. Chip photograph of the 800-MHz QT VCO.

A. An 800-MHz Adaptive VCO

Serving as a proof of concept, an adaptive VCO has been designed that can trade performance, i.e., phase noise, for power consumption and thereby can be adapted to varying radio-channel conditions. An adaptive VCO [16] for use in the 800-MHz band is designed for a phase-noise tuning range of $\rm PNTR = 7$ dB with a factor 3.3 saving in power consumption. The oscillator employs the topology shown in Fig. 1, with base biasing $V_B = V_{\rm CC}$ and a tail-current source degenerative resistance $Z_D = R_D$.

For a quasi-tapping ratio of $n = 2$, quasi-tapping capacitances $C_\pi + 2C_A = 1$ pF and $2C_B = 1$ pF have been chosen, C_π being the base–emitter capacitance of active devices Q_1 and Q_2 adding to capacitance $2C_A$ (see Fig. 1). For the variable capacitor (varactor), a reverse biased base-collector junction has been employed. Optimized for low-power operation, a rather large inductance value of 12 nH is chosen, laid-out in 1 um thick second metal layer. A two-stage common-collector buffer has been used as interfacing stage between the VCO and measurement equipment. The sizing of the oscillator parameters has been done in accordance with the design for adaptivity procedure, while the optimization of the oscillator performance has been done with the aid of the *phase-noise-inductance* simulator [17]. A good match is obtained between the results predicted by calculations and simulations on one the hand and the measurement results on the other, emphasizing the merit of the undertaken design procedure.

The chip micrograph of the QT VCO is shown in Fig. 4. It occupies an area of 1 mm^2, including bondpads. Wirebonded on a 20-lead package, it is placed in a metal test fixture where the measurements have been performed.

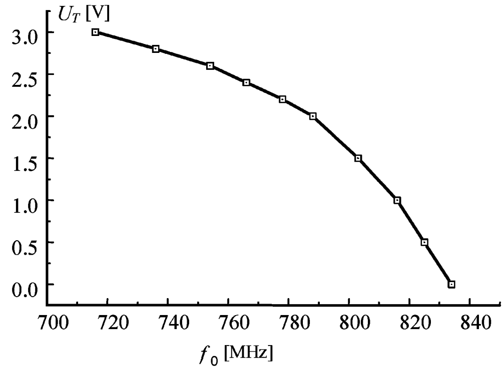

Fig. 5. Frequency tuning range of the QT VCO.

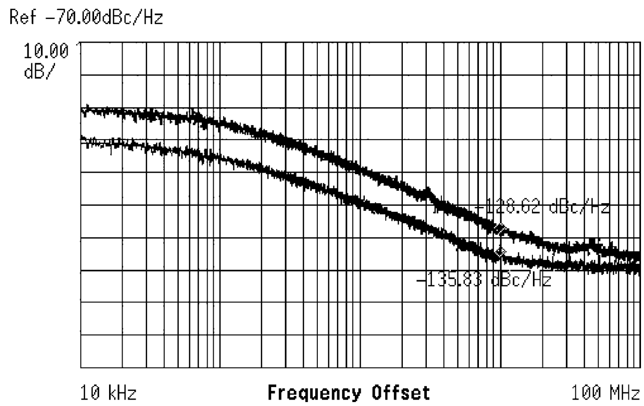

Fig. 6. Maximum and minimum phase noise at 10-MHz offset from 800-MHz oscillating frequency at tail-current levels of 5 and 1.5 mA.

For a 3-V tuning voltage, a frequency tuning range of 120 MHz, between 715 and 835 MHz, is achieved. The measured frequency tuning range is shown in Fig. 5.

Using the devices that have been available in the employed technology, characterized by the maximal transit frequency $f_T = 8$ GHz, the VCO achieves a phase noise of $-$ 135.8 dBc/Hz at 10-MHz offset from the 800-MHz oscillation frequency at a current consumption level of 5 mA from a 3-V supply. At a current consumption level of 1.5 mA, the oscillator achieves a phase noise of $-$ 128.6 dBc/Hz at 10-MHz offset frequency from the 800-MHz oscillation frequency. The plots of the maximal and the minimal phase noise are shown in Fig. 6. The achieved phase-noise difference of 7 dB trades with a factor 3.3 reduction in power consumption.

In this single-standard application, the provided adaptivity is utilized as a *power saving mechanism*, thereby enhancing the oscillator performance.

The need for the frequency-transconductance tuning is depicted in Fig. 7, where the spectrum of the oscillator's output signal is shown.

Here, the oscillator is tuned to the resonant frequency $f_1 =$ 800 MHz at a tail-current level $I_{\mathrm{TAIL}} = 2.5$ mA. The measured signal power is $-$ 19 dBm, corresponding to a loop gain value $k = 3$. By tuning the resonant frequency to f_2 =740-MHz the oscillation signal output power changes to $-$ 26 dBm, and oscillator loop gain to $k = 1$. Any further reduction in frequency, at the same power consumption level, results in a disappearance

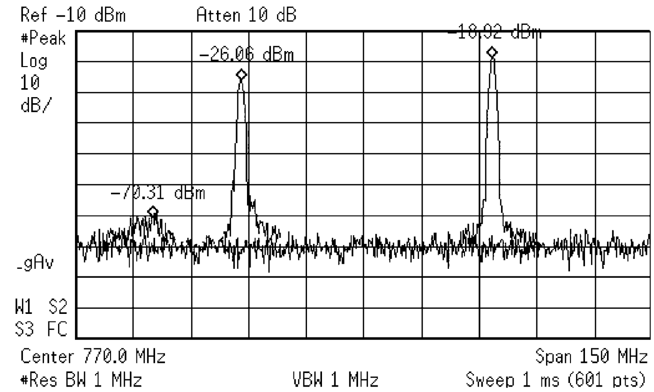

Fig. 7. Frequency-transconductance tuning from 800- to 715-MHz oscillating frequency at 2.5-mA tail current level.

of the oscillations as the oscillation condition doesn't hold any more, i.e., $k < 1$. This is shown in Fig. 7 at left.

B. Application of Adaptivity to MultiStandard Designs

Demands for new telecom services requiring higher capacities and higher data rates have motivated the development of broadband, third-generation wireless systems. The coexistence of second and third generation cellular systems requires multimode, multiband, and multistandard mobile terminals.

Multistandard front-ends typically use duplicate circuit blocks, or even entire radio front-ends for each standard. Although this approach is simpler to implement, it is neither optimal in cost nor in power consumption [3].

Another solution is a design that satisfies the most stringent specification of the most demanding standard. However, such designs consume more power than necessary when operating under more relaxed conditions of the less demanding standards [18].

To prolong talk-time, it is desirable to *share* circuit functions across multiple standards in these multifunctional handsets. This can be achieved by using *adaptive circuits* that are able to trade off power consumption for performance on the fly [19].

Adaptive RF circuits allow for reduced area, power consumption, and most importantly lower cost in both single-standard and multistandard terminals.

VI. Conclusion

Frequent changes of conditions under which communication systems of today operate necessitate new design philosophy of analog RF front-end circuits. Therefore, a concept of design for adaptivity is introduced in this paper, establishing a procedure for performance characterization of adaptive oscillators with an explicit qualitative and quantitative description of the relationships and tradeoffs between the oscillator performance parameters.

First, the presented concept of phase-noise tuning has explained how oscillators can trade performance for power consumption in an adaptive way. It has been shown what are the extremes of the phase-noise tuning range and the power consumption saving.

Furthermore, the concept of frequency-transconductance tuning has been presented. The derived analytical expressions show how this concept can be employed in order to achieve full control over the operation of the oscillator that is changed as a result of frequency tuning.

Finally, an 800-MHz adaptive voltage controlled oscillator design has been described as a proof-of-concept, allowing for a phase-noise tuning range of 7 dB and more than a factor three saving in power consumption.

ACKNOWLEDGMENT

The authors thank National Semiconductors—Delft Design Center, The Netherlands, for fabrication access.

REFERENCES

[1] A. Abidi *et al.*, "Power-conscious design of wireless circuits and systems," *Proc. IEEE*, vol. 88, no. 10, pp. 1528–1545, Oct. 2000.

[2] F. Bruccoleri *et al.*, "Noise cancelling in wide-band CMOS LNAs," in *Proc. ISSCC*, Feb. 2002, pp. 406–407.

[3] J. Ryynanen, K. Kivekas, J. Jussila, A. Parssinen, and K. Halonen, "A dual-band RF front-end for WCDMA and GSM applications," in *Proc. CICC*, May 2000, pp. 175–178.

[4] A. Ham and A. Hajimiri, "Concepts and methods in optimization of integrated *LC* VCOs," *IEEE J. Solid-State Circuits*, vol. 36, no. 6, pp. 896–909, Jun. 2001.

[5] A. Hajimiri and T. H. Lee, "A general theory of phase noise in electrical oscillators," *IEEE J. Solid-State Circuits*, vol. 33, no. 2, pp. 179–194, Feb. 1998.

[6] A. Tasić and W. A. Serdijn, "Concept of phase-noise tuning of bipolar voltage-controlled oscillators," in *Proc. ISCAS*, May 2002, pp. 161–164.

[7] ——, "Concept of frequency-transconductance tuning of bipolar voltage-controlled oscillators," in *Proc. ISCAS*, May 2002, pp. 26–29.

[8] C. van den Bos *et al.*, "Architecture of a reconfigurable radio receiver front-end using overall feedback," in *Proc. PRORISC*, Nov. 2001.

[9] A. Tasić and W. A. Serdijn, "Concept of quasi-capacitive tapping of bipolar voltage-controlled oscillators," in *Proc. ICECS*, May 2002, pp. 15–18.

[10] R. Aparicio and A. Hajimiri, "A noise-shifting differential colpitts VCO," *IEEE J. Solid-State Circuits*, vol. 37, no. 12, pp. 1728–1736, Dec. 2002.

[11] A. Tasić, W. A. Serdijn, and J. R. Long, "Low-noise biasing of voltage-controlled oscillator's by means of resonant-inductive degeneration," in *Proc. ISCAS*, May 2003, pp. 673–373.

[12] J. Craninx and M. Steyaert, "Low-noise voltage-controlled oscillators using enhanced *LC* tanks," *IEEE Trans. Circuits Syst. II, Analog Digit. Signal Process.*, vol. 42, no. 12, pp. 792–804, Dec. 1995.

[13] A. Tasić and W. A. Serdijn, "K-Rail diagrams—Comprehensive tool for full performance characterization of voltage-controlled oscillators," in *Proc. ICECS*, Sep. 2002, pp. 15–18.

[14] B. Razavi, *RF Microelectronics*. Upper Saddle River, NJ: Prentice-Hall, 1998.

[15] J. Craninx and M. Steyaert, "A 1.8-GHz low-phase-noise CMOS VCO using optimal hollow spiral inductors," *IEEE J. Solid-State Circuits*, vol. 32, no. 5, pp. 736–744, May 1997.

[16] A. Tasić, W. A. Serdijn, and J. R. Long, "800-MHz voltage-controlled oscillator with 6 dB phase-noise tuning range," in *Proc. MIEL*, May 2004, pp. 559–562.

[17] ——, "Effects of substrate on phase noise of voltage-controlled oscillators," in *Proc. ISCAS*, May 2002, pp. 26–29.

[18] D. Wang *et al.*, "A fully integrated GSM/DCS/PCS Rx VCO with fast switching auto-band selection," in *Proc. RAWCON*, Aug. 2002, pp. 209–212.

[19] A. Tasić, W. A. Serdijn, and J. R. Long, "DCS1800/WCDMA—Adaptive voltage-controlled oscillator," in *Proc. ISCAS*, May 2004, pp. 177–180.

Aleksandar Tasić received the M.Sc. (engineer) degree in electrical engineering from the Electronics Faculty, University of Nis, Nis, Serbia, in 1998. Since 2000, he is working toward the Ph.D. degree in electronics at the Delft University of Technology, Delft, The Netherlands.

He was with the Electronics Faculty, University of Nis until 2000. His research interest includes the design of adaptive and multistandard RF front-end circuits for wireless communications and RF front-end system study for optimal selection of specifications for receiver building blocks.

Wouter A. Serdijn was born in Zoetermeer, The Netherlands, in 1966. He and received the "ingenieurs" (M.Sc.) degree and the Ph.D. degree from the Delft University of Technology, Delft, The Netherlands, in 1989, and in 1994, respectively.

Since 2002, Dr. Serdijn is a Workpackage Leader in the Freeband Impulse Project AIR-LINK, aiming at high-quality, wireless short-distance communication, employing ultra-wide band (UWB) radio. His research interests include low-voltage, ultra-low-power, high-frequency and dynamic-translinear analog integrated circuits along with circuits for RF and UWB wireless communications, hearing instruments and pacemakers. He teaches analog electronics for electrical engineers, micropower analog integrated circuit techniques and electronic design techniques. He is co-editor and coauthor of the books *Research Perspectives on Dynamic Translinear and Log-Domain Circuits* (Norwell, MA: Kluwer, 2000), *Low-Voltage Low-Power Analog Integrated Circuits* (Norwell, MA: Kluwer, 1995), and *Dynamic Translinear and Log-Domain Circuits* (Norwell, MA: Kluwer, 1998). He authored and co-authored more than 150 publications and presentations.

Dr Serdijn has served as an Associate Editor of the IEEE TRANSACTIONS ON CIRCUITS AND SYSTEMS—II: ANALOG DIGITAL SIGNAL PROCESSING, as Tutorial Session Co-Chair for the International Symposium on Circuits and Systems (ISCAS) 2003, as Analog Signal Processing Track Co-Chair, for ISCAS 2004, as Chair of the Analog Signal Processing Technical Chapter of the IEEE CAS society, and currently serves as an Associate Editor of the IEEE TRANSACTIONS ON CIRCUITS AND SYSTEMS—I: REGULAR PAPERS, as Analog Signal Processing Track Co-Chair for ICECS 2004, as Technical Program Committee member for the 2004 International Workshop on Biomedical Circuits and Systems, and as Analog Signal Processing Track Co-Chair for ISCAS 2005.

John R. Long received the B.Sc. degree in electrical engineering from the University of Calgary, Calgary, AB, Canada, in 1984, and the M.Eng. and Ph.D. degrees in electronics engineering from Carleton University, Ottawa, ON, Canada, in 1992 and 1996, respectively.

He was employed for 10 years by Bell-Northern Research, Ottawa (now Nortel Networks) involved in the design of ASICs for gigabit/s fiber-optic transmission systems and for 5 years at the University of Toronto, Toronto, Canada. He joined the faculty at the Delft University of Technology, Delft, The Netherlands, in January 2002 as Chair of the Electronics Research Laboratory. His current research interests include low-power transceiver circuitry for highly-integrated radio applications, and electronics design for high-speed data communications systems.

Prof. Long is currently serving on the Technical Program Committees of the International Solid-State Circuits Conference (ISSCC), the European Solid-State Circuits Conference (ESSCIRC), the IEEE Bipolar/BiCMOS Circuits and Technology Meeting (BCTM), and GAAS2004 (EuMW). He is a former Associate Editor of the IEEE JOURNAL OF SOLID-STATE CIRCUITS. He received the NSERC Doctoral Prize and Douglas R. Colton and Governor General's Medals for research excellence, and Best Paper Awards from ISSCC 2000 and IEEE-BCTM 2003.